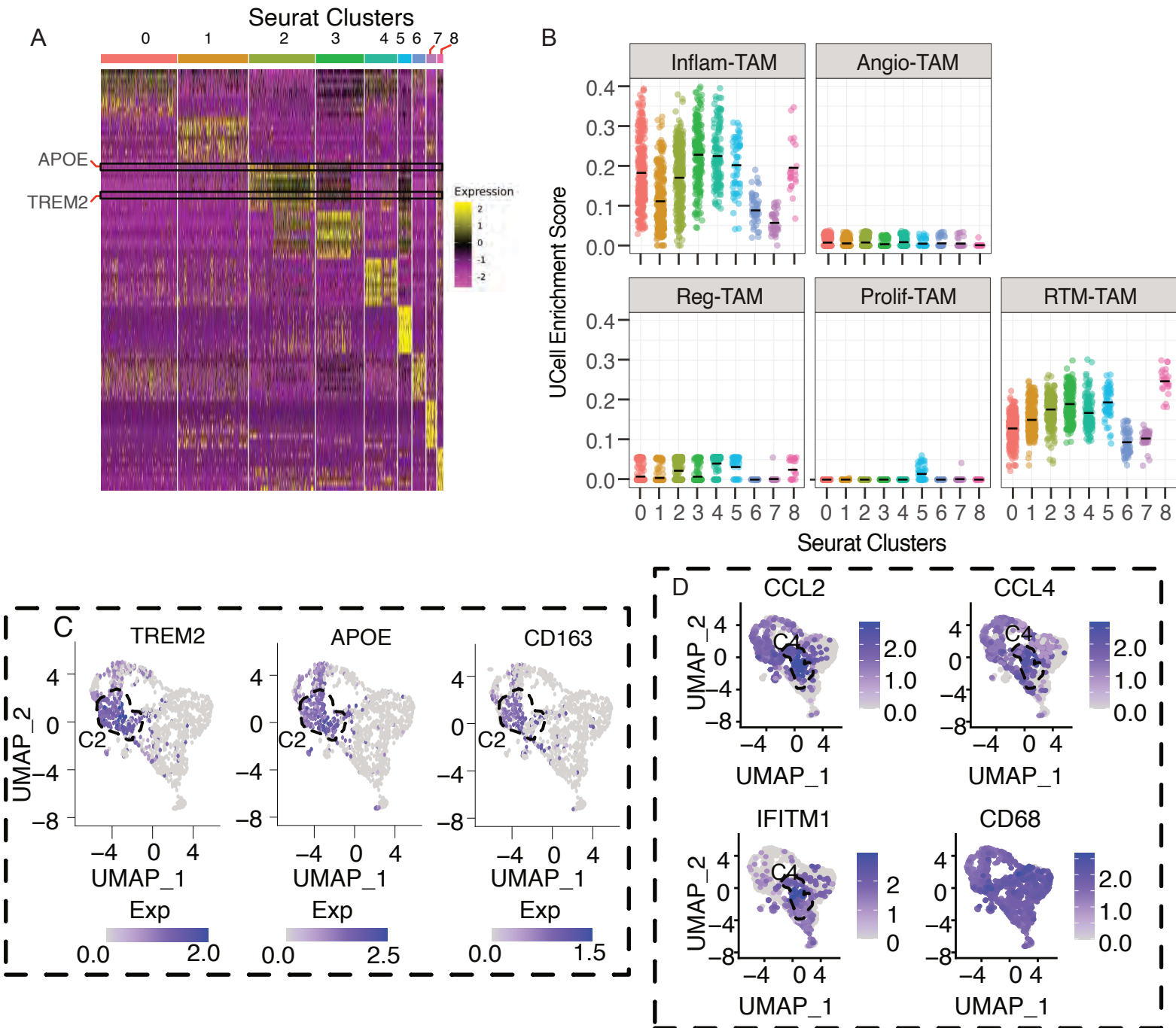


Fig S1



**Fig. S1: Identification of functionally opposing TAM states**

(A) Differential gene expression analysis across the macrophage clusters is shown as a heatmap where macrophage clusters are annotated as columns. Two representative genes (APOE and TREM2) highly expressed in C2 are highlighted by a black box. Color code indicates levels of gene expression, whereas yellow and purple represent high and low expressions, respectively.

(B) UCell enrichment score of TAMs (Inflam-TAM, Angio-TAM, Reg-TAM, Prolif-TAM, and RTM-TAM) are shown as a jitter plots.

(C and D) UMAP showing the expression of LA-TAM markers (TREM2, APOE, CD163) (C), IFN-TAM markers (CCL2, CCL4, and IFITM1) (D), and macrophage marker gene (CD68) (D). The C2 (C) and C4 (D) population is demarcated by a black dashed line.

Fig S2

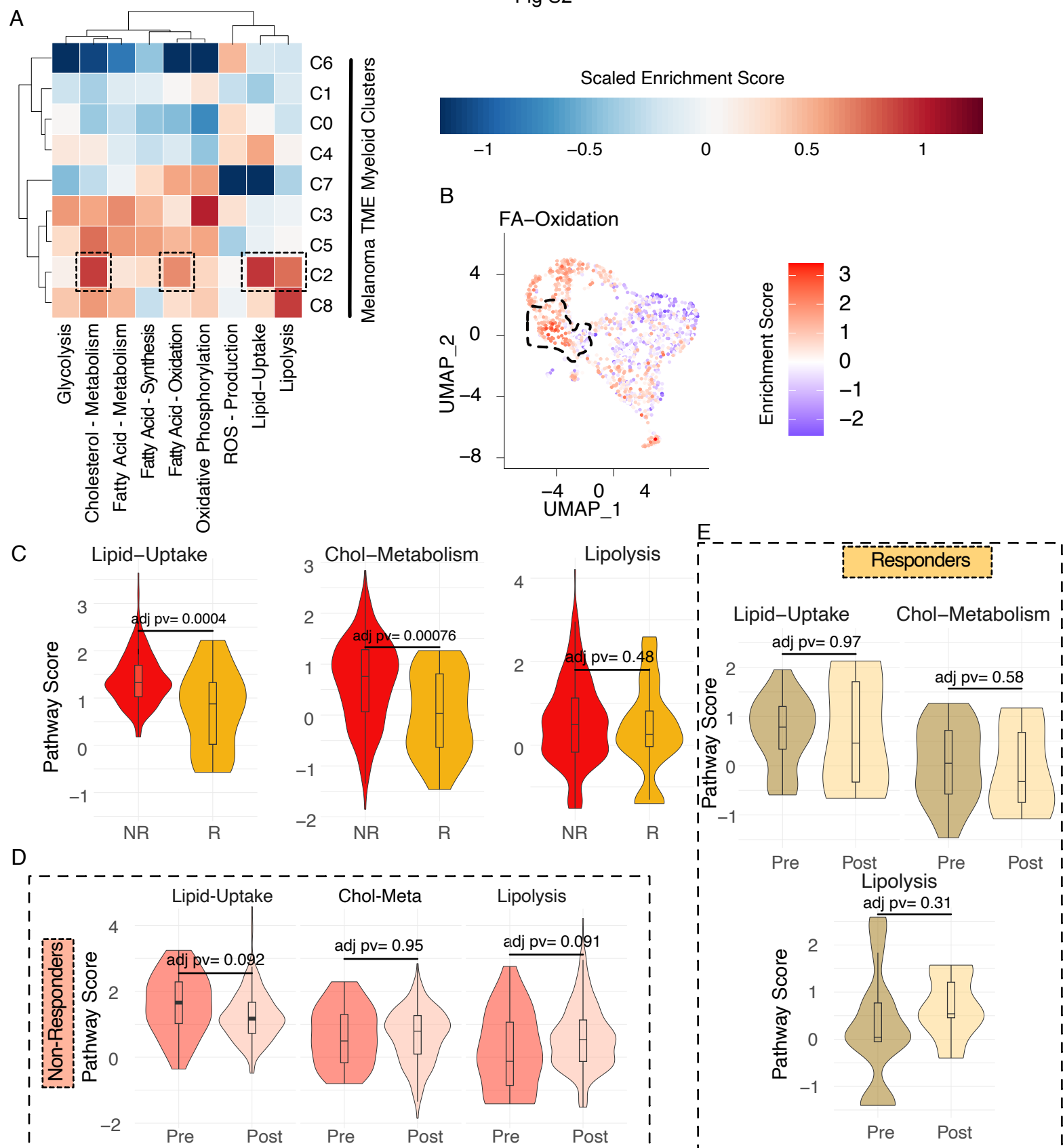


**Fig. S2: Lipid metabolism landscape in macrophages**

(A) Enrichment of lipid metabolism associated gene sets (Lipid-Uptake, Cholesterol Metabolism, and Lipolysis) across macrophage population. Enrichment based on the Univariate Linear Model (ULM) is mapped in UMAP space. Color code represents the Enrichment score. (B) Single-cell UCell enrichment score of the gene signatures representing FA-oxidation mapped onto UMAP space. The dashed line demarcates the boundary of cluster 2 (C). Comparison of pathway enrichment score of Lipid-Uptake, Cholesterol Metabolism (Chol-Metabolism), and Lipolysis between Non-Responders (NR) and Responders (R). Adjusted p-values (adj pv) are given. (D) Comparison of pathway enrichment score between pre- and post-treatment time points in Non-Responders. (E) Comparison of pathway enrichment score between pre- and post-treatment time points in Responders.

Fig S3

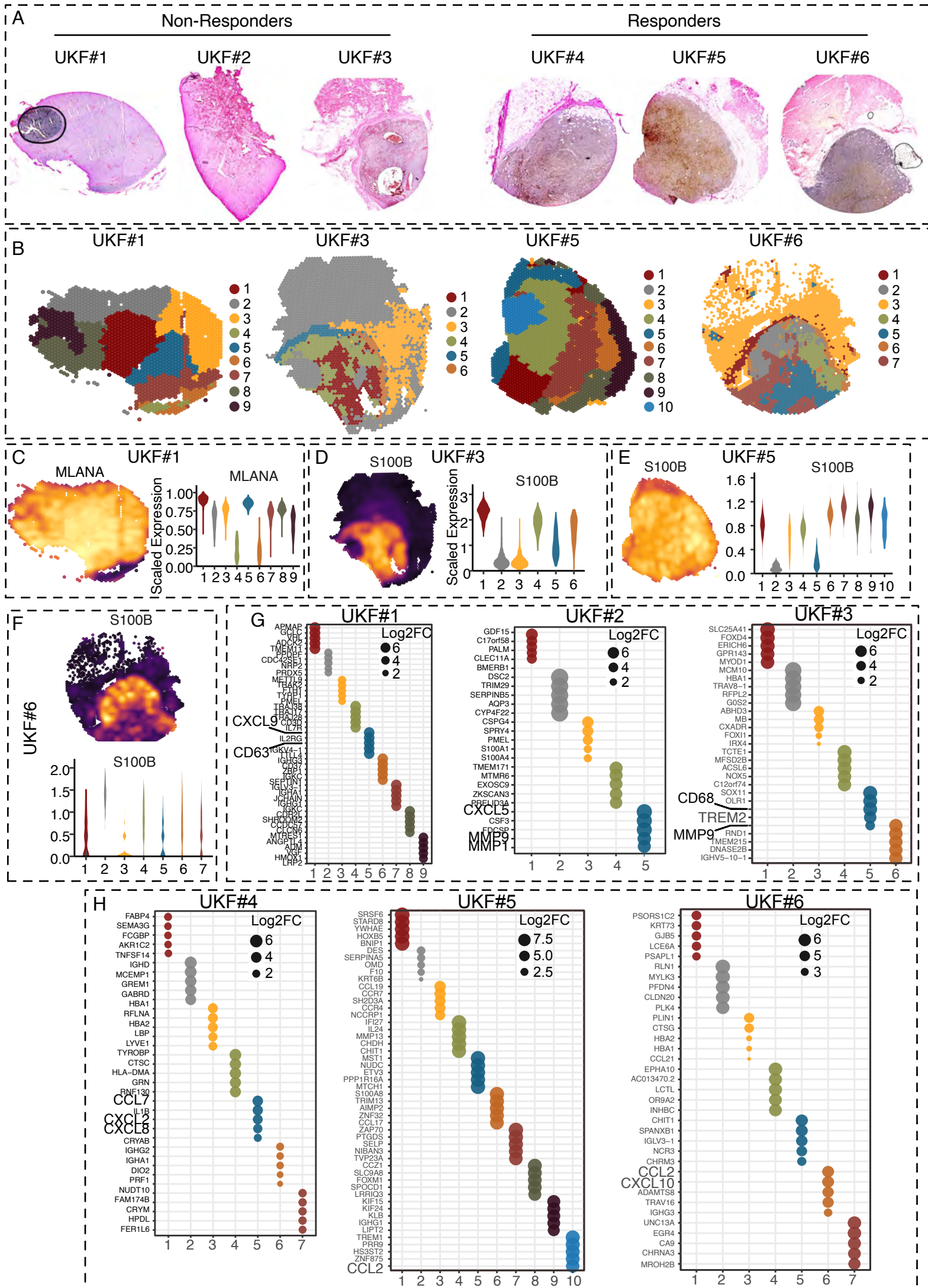


**Fig. S3: Spatial characterization of the immune and tumor microenvironment in metastatic melanoma patients undergoing ICI therapy**

(A) H&E-stained tissue sections of ICI Non-Responder (UKF#1, UKF#2, and UKF#3) and Responder (UKF#4, UKF#5, and UKF#6) patients with metastatic melanoma. (B) BayesSpace clustering based on the spatial transcriptome data from UKF#1, UKF#3, UKF#5, and UKF#6 is shown. (C-F) The spatial and cluster-wise expression of the canonical melanoma markers (MLANA and S100B) in UKF#1 (C), UKF#3 (D), UKF#5 (E), and UKF#6 (F) are shown as surface plots. For surface plots, the color code represents the relative gene expression. (G and H) Cluster-wise expressions of DEGs (Differentially Expressed Genes, shown as Log<sub>2</sub>FC) are depicted for Non-Responder (UKF#1, UKF#2, and UKF#3) (G), and Responder (UKF#4, UKF#5, and UKF#6) (H) patients.

Fig S4

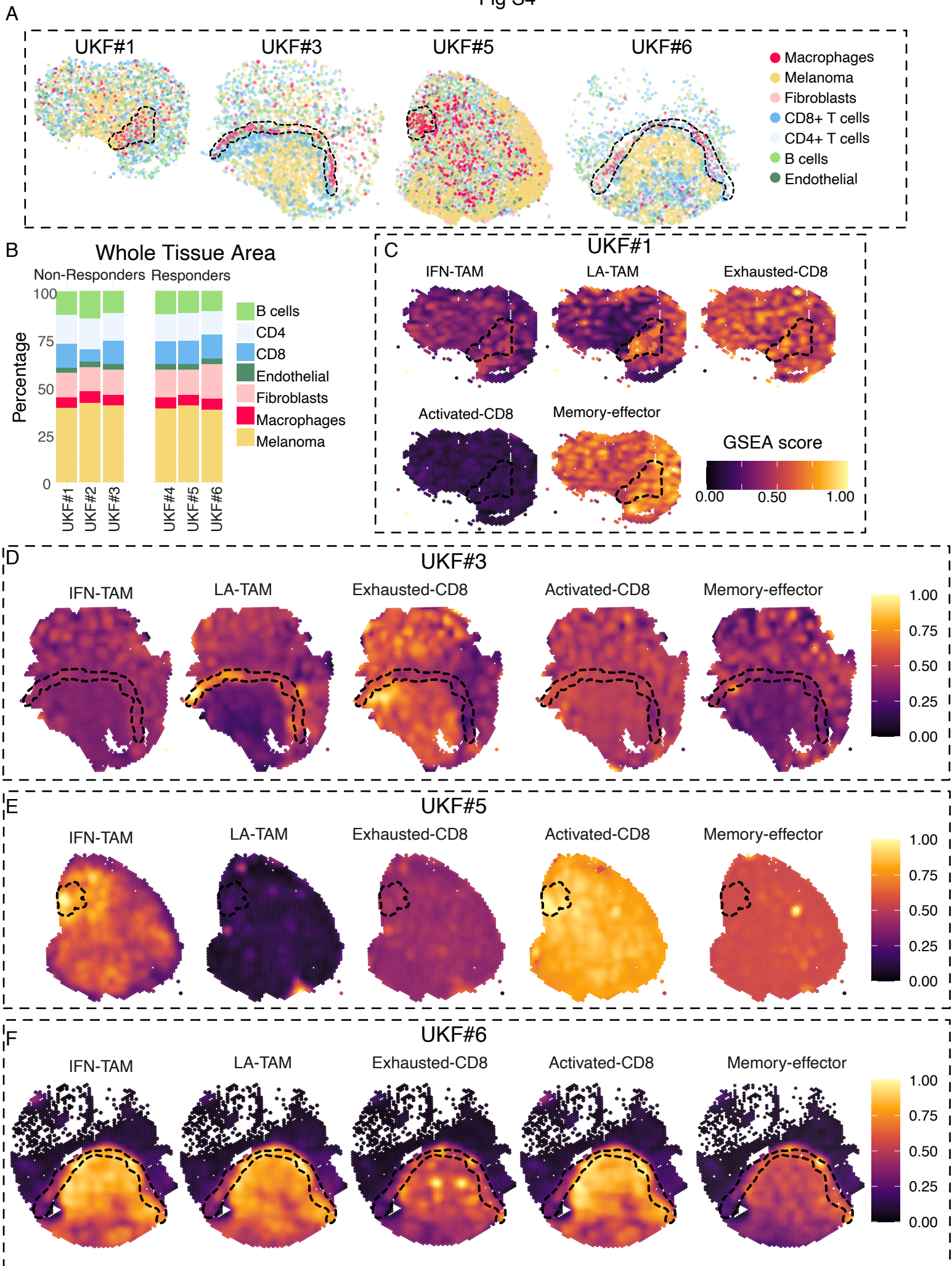


**Fig. S4: Deconvolution of spatial transcriptomics data reveals immune and tumor cell heterogeneity in metastatic melanoma**

(A) Deconvolution of spatial spots into single-cells by assigning single-cell transcriptome profiles from Tirosh *et al.* to in situ spatial transcriptomics (ST) data from patient UKF#1, UKF#3, UKF#5, and UKF#6. The cell types (Macrophages, Melanoma, Fibroblast, CD8<sup>+</sup> T cell, CD4<sup>+</sup> T cell, B cell, and Endothelial cells) are indicated by color code. The myeloid-enriched regions are indicated by a black dashed line. (B) The percentages of different cell types in the whole tissue sections across Non-Responder and Responder patients are represented as stacked bar plots. (C-F) GSEA of selected gene signatures representing IFN-TAMs, LA-TAMs, Exhausted-CD8, Activated-CD8, and Memory-effector cells are illustrated by surface plots for UKF#1 (C), UKF#3 (D), UKF#5 (E), and UKF#6 (F) where GSEA score is depicted by color code. Myeloid-enriched regions are marked with dashed lines.

Fig S5

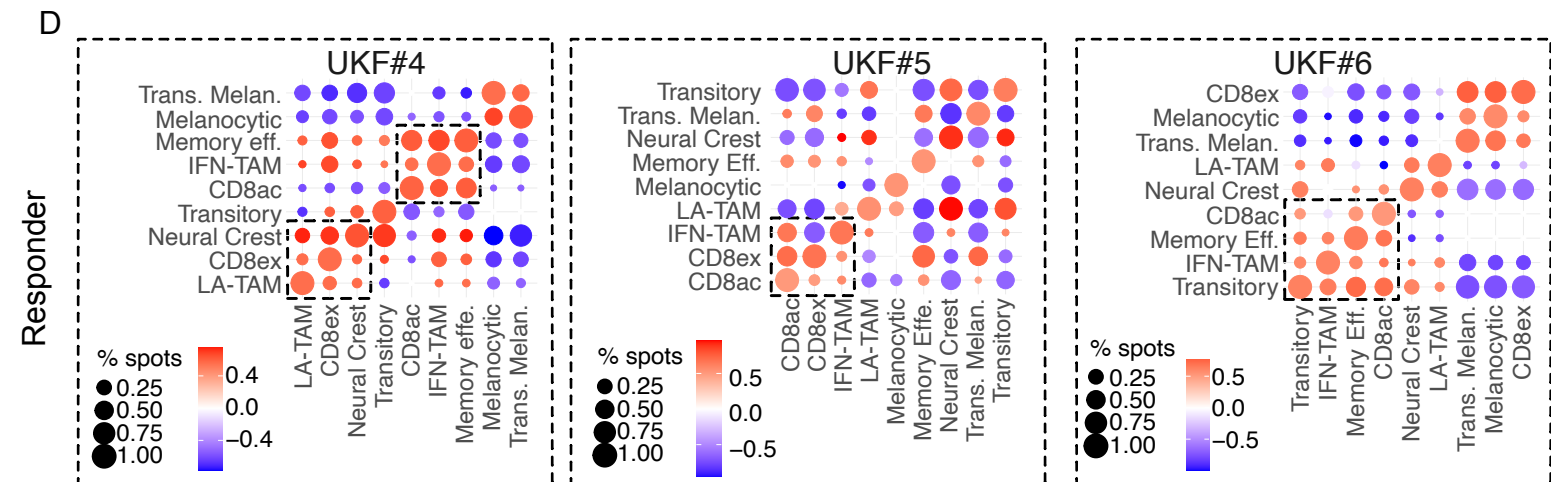
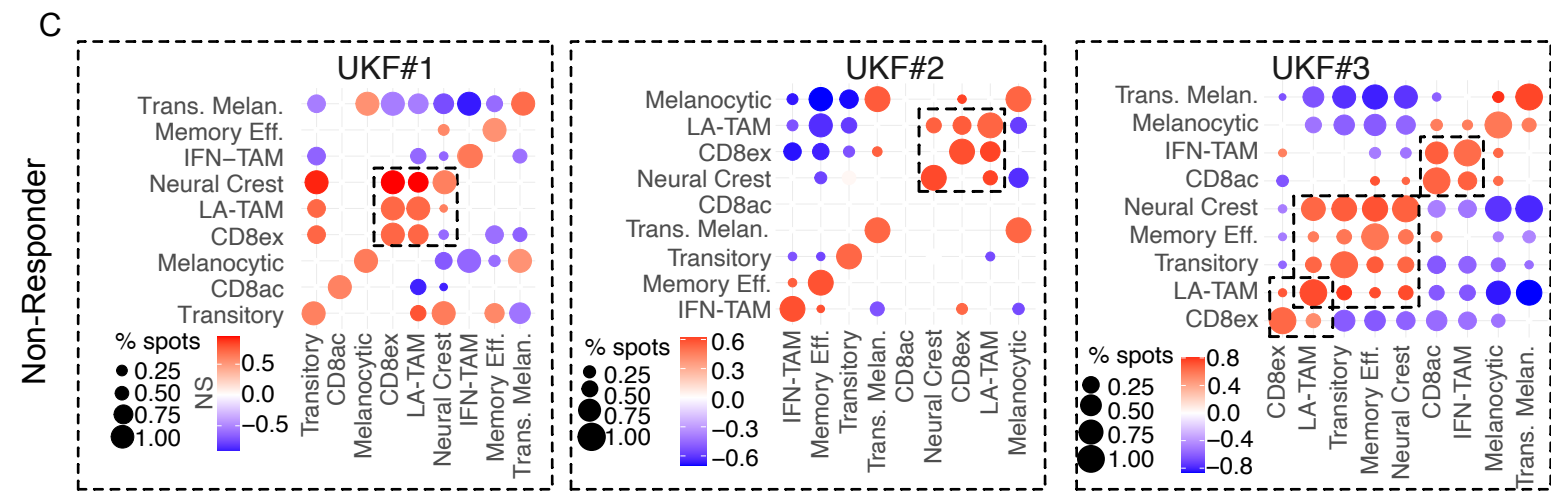
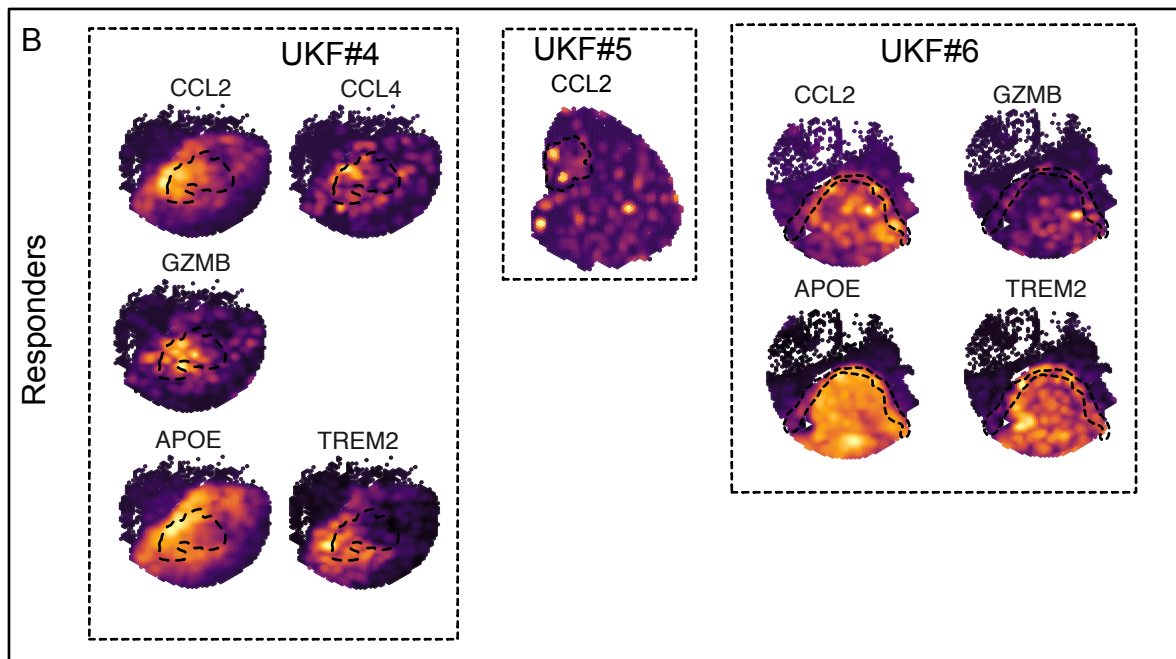
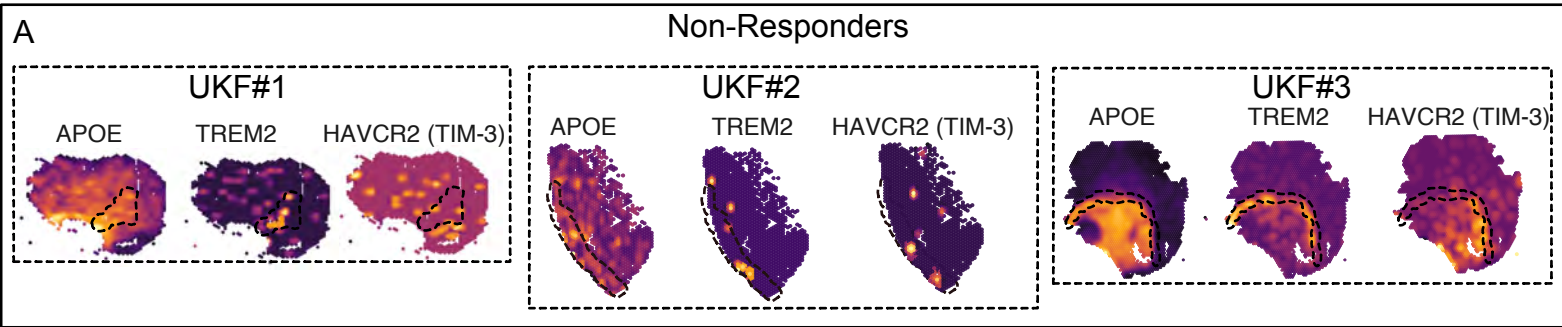


**Fig. S5: Neighborhood analysis of tumor-associated macrophages and CD8<sup>+</sup> T cell subsets in metastatic melanoma**

(A) Spatial expression of LA-TAM markers (APOE, TREM2), and Exhausted-CD8 marker (TIM3/HAVCR2) are shown across Non-Responder patients (UKF#1, UKF#2, and UKF#3). (B) IFN-TAM markers (CCL2, CCL4) and Activated-CD8 cell marker (GZMB) are shown in the tissue section of Responder patients (UKF#4, UKF#5, and UKF#6). For UKF#5, only CCL2 expression was observed. The myeloid-enriched tissue region within the tissue is highlighted by a dashed line. (C and D) Neighborhood analysis was performed to quantify the distance among the spots enriched with two different gene signatures and estimate the spatial co-localization probability of the gene signatures. The results are represented as a dot plot for Non-Responder (C) and Responder patients (D). The gene sets in the rows are anchors, illustrating that anchor spatial spots are selected with respect to these anchor gene signatures (rows), whereas the columns indicate the neighborhood corresponding to the spatial overlap of these gene signatures with respect to anchor spots. The higher score (red) indicates the co-localization, whereas the lower score (blue) indicates that the gene signatures are distinctly located (non-overlapping). The size of the indicates the fraction of the spatially-colocalized spots.

Fig S6

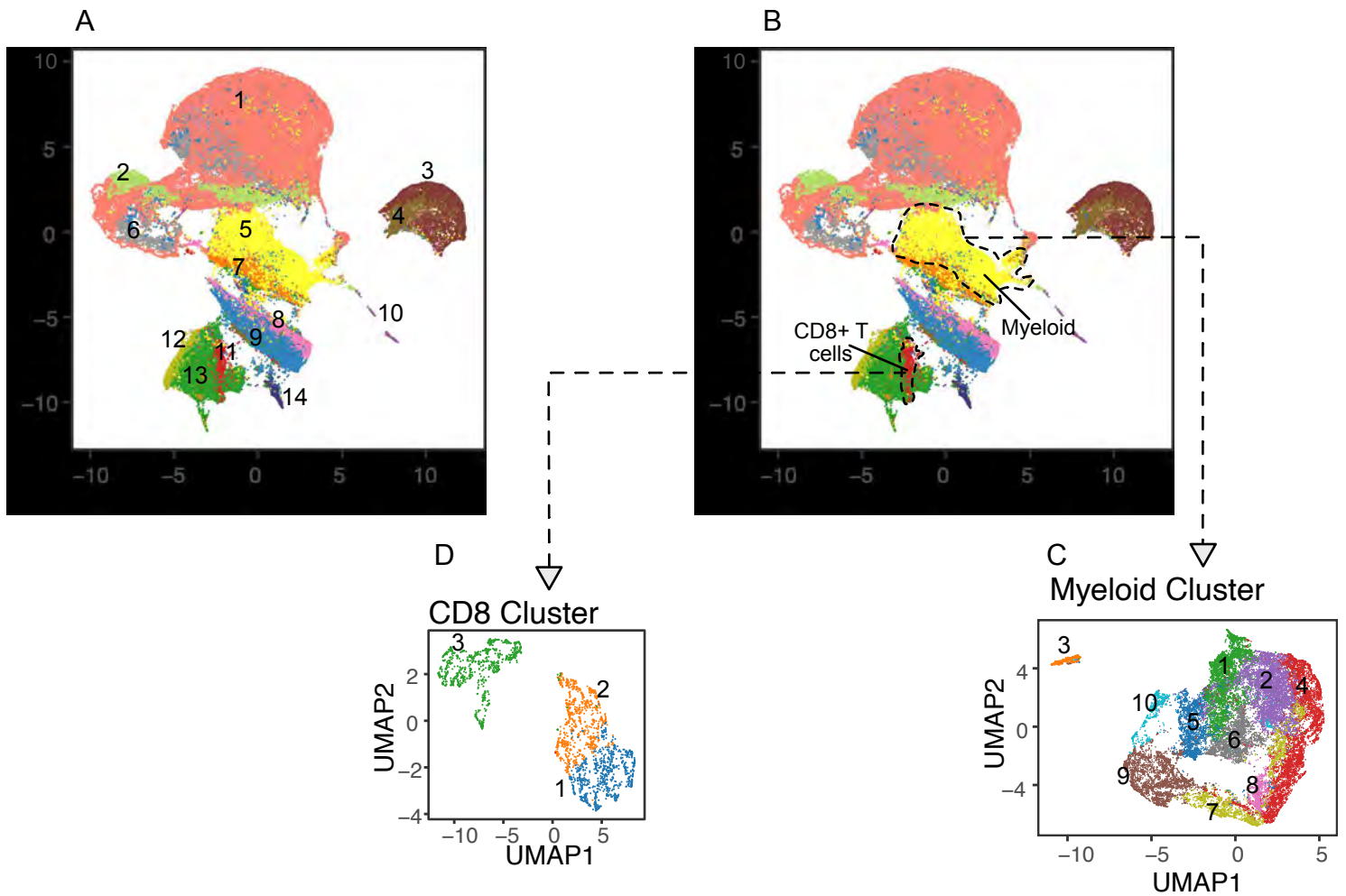


**Fig. S6: Single-cell protein expression profiling of immune and tumor microenvironment in metastatic melanoma patients**

(A) UMAP representation of single-cell IMC data, illustrating the distribution of different clusters. (B) UMAP showing the Myeloid and CD8<sup>+</sup> T cell clusters highlighted by the dashed line. These two populations of cells were used for further sub-clustering. (C) The subclustering of the Myeloid cells resulted in 10 clusters. (D) Sub-clustering of CD<sup>+</sup> T cells, yielding 3 different clusters, is shown.

Fig S7

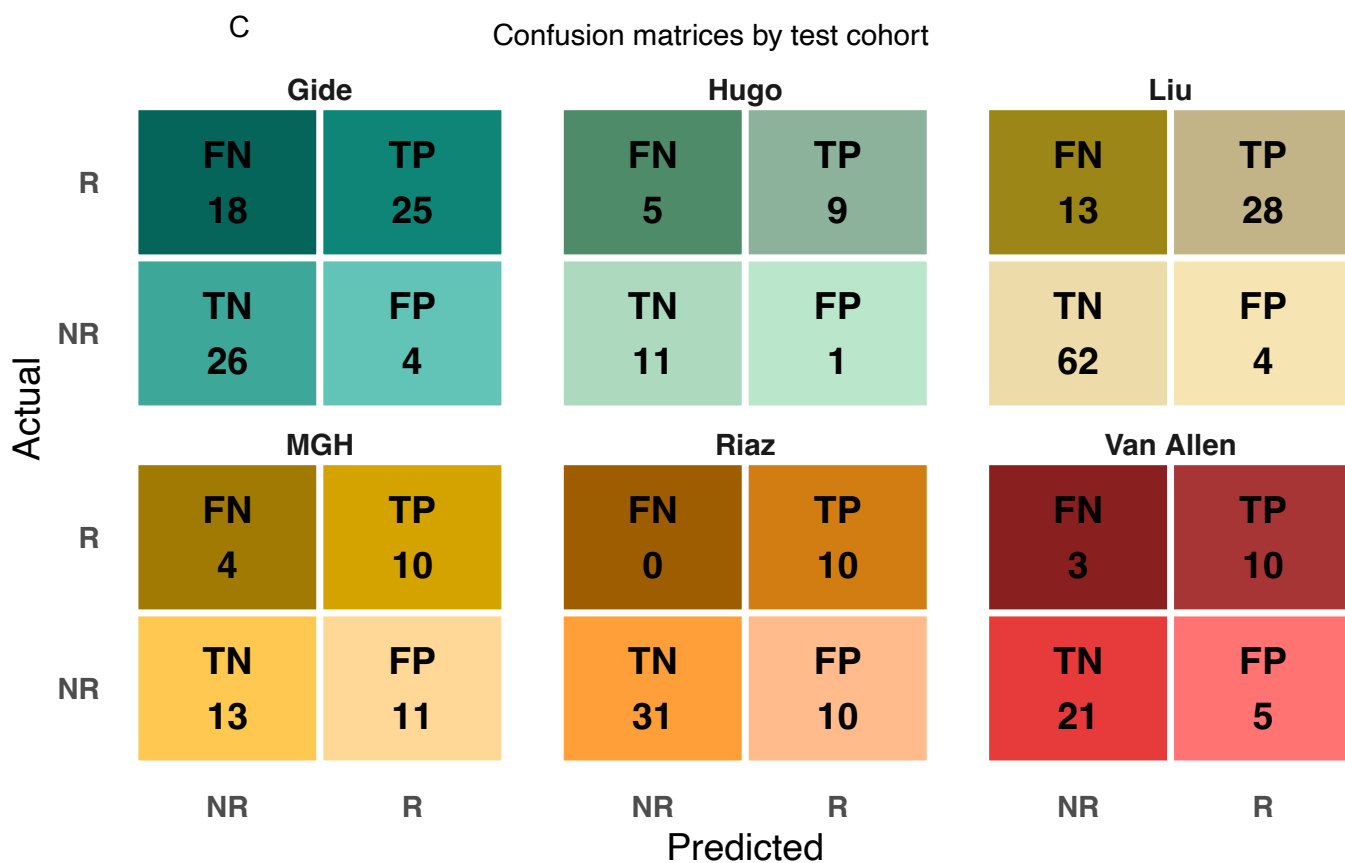
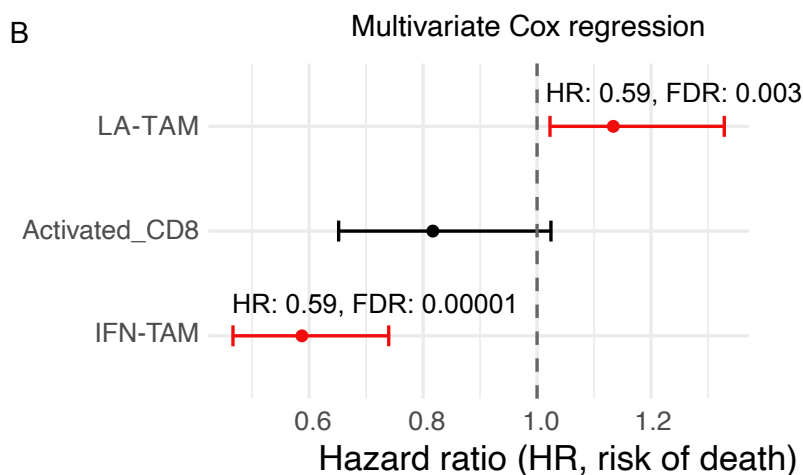
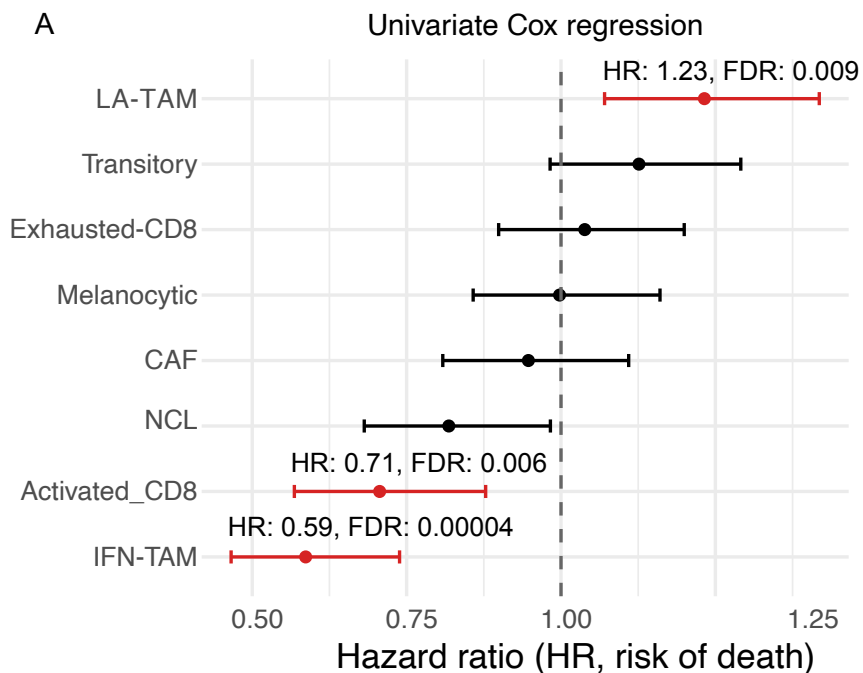


**Fig. S7: Immune state classification of pre-ICI cohort**

(A) A forest plot representing the hazard ratios (HRs) and false discovery rates (FDRs) of different features across the pretreatment cohort calculated by univariate analysis is shown. HRs are shown with 95% CI. Features with a significant FDR were marked in red. (B) A forest plot for multivariate analysis is shown. Features with a significant FDR were marked in red. For multivariate analysis, only the factors that were significantly associated with survival outcomes in univariate analysis were included. Adjustment for confounding factors such as cohort and therapy type was performed. Features with significant FDR were marked in red. (C) The confusion matrices for each validation cohort are shown, where the x-axis and y-axis represent the predicted and real outcomes. FN = False Negative; TP = True Positive; TN = True Negative; FP = False Positive.